ARTICLE

EGF-mediated induction of Mcl-1 at the switch to lactation is essential for alveolar cell survival

Nai Yang Fu[1,2], Anne C. Rios[1,2,10], Bhupinder Pal[1,2,10], Rina Soetanto[3], Aaron Lun[2,4], Kevin Liu[1,2], Tamara Beck[1,2], Sarah A. Best[1,2], François Vaillant[1,2], Philippe Bouillet[2,5], Andreas Strasser[2,5], Thomas Preiss[3,6], Gordon K. Smyth[4,7], Geoffrey J. Lindeman[1,8,9,10], Jane E. Visvader[1,2,10,11]

[1]Stem Cells and Cancer Division, The Walter and Eliza Hall Institute of Medical Research, Parkville, Victoria 3052, Australia. [2]Department of Medical Biology, The University of Melbourne, Parkville, Victoria 3010, Australia. [3]Genome Biology Department, The John Curtin School of Medical Research, The Australian National University, Canberra, ACT 0200, Australia. [4]Bioinformatics Division, The Walter and Eliza Hall Institute of Medical Research, Parkville, Victoria 3052, Australia. [5]Molecular Genetics of Cancer Division, The Walter and Eliza Hall Institute of Medical Research, Parkville, Victoria 3052, Australia. [6]Victor Chang Cardiac Research Institute, Darlinghurst, NSW 2010, Australia. [7]Department of Mathematics and Statistics, The University of Melbourne, Parkville, Victoria 3010, Australia. [8]Department of Medical Oncology, The Royal Melbourne Hospital, Parkville, Victoria 3050, Australia. [9]Department of Medicine, The University of Melbourne, Parkville, Victoria 3010, Australia.

[10]These authors contributed equally to this work

[11]Correspondence should be addressed to J.E.V. (e-mail: visvader@wehi.edu.au)

Expansion and remodeling of the mammary epithelium requires a tight balance between cellular proliferation, differentiation and death. To explore cell survival versus cell death decisions in this organ, we deleted the pro-survival gene *Mcl-1* in the mammary epithelium. *Mcl-1* was found to be essential at multiple developmental stages including morphogenesis in puberty and alveologenesis in pregnancy. Moreover, *Mcl-1*-deficient basal cells were virtually devoid of repopulating activity, suggesting that this gene is required for stem cell function. Profound upregulation of Mcl-1 protein was evident in alveolar cells at the switch to lactation, and *Mcl-1* deficiency impaired lactation. Interestingly, *EGF* was identified as one of the most highly upregulated genes upon lactogenesis and inhibition of EGF or mTOR signalling markedly impaired lactation, with concomitant decreases in Mcl-1 and phosphorylated ribosomal protein S6. These data demonstrate that Mcl-1 is essential for mammopoiesis and identify EGF as a critical trigger of Mcl-1 translation to ensure survival of milk-producing alveolar cells.

Unlike most tissues, the mammary gland exists as a rudimentary tree at birth and predominantly develops in the postnatal animal[1]. Morphogenesis during puberty is characterized by ductal elongation and branching to form an elaborate ductal tree, which comprises an inner layer of luminal cells and an outer layer of myoepithelial cells adjacent to the basement membrane. During pregnancy, the mammary epithelium undergoes massive expansion, with the formation of alveolar structures that terminally differentiate into secretory units in late pregnancy to enable lactation. Following weaning, these alveolar structures regress via programmed cell death, thus returning the gland to a virgin-like state. Two major forms of cell death have been implicated in the involution process, apoptosis[2] and more recently, lysosomal-mediated death[3] that occurs independently of caspases[3]. However, the molecular regulators that control cell death versus survival decisions in the mammary gland are poorly defined.

The Bcl-2 protein family members act as the arbiters of the intrinsic apoptotic pathway[4,5] and comprise pro-survival members (e.g. Bcl-2, Mcl-1, Bcl-X_L), initiators of apoptosis (e.g. Bim), and the downstream effector proteins Bak and Bax. Whether or not any member of the Bcl-2 family plays an essential role in the mammary gland remains an important question. Loss of *Bcl-x*[6] causes mild abnormalities in involution, while loss of *Bim*[7] is associated with a transient phenotype in puberty, in which clearing of the luminal space of terminal endbuds and terminal ducts was delayed. In other tissues, the pro-survival protein Mcl-1 has been shown to be critical for the survival of diverse cell types, including hematopoietic stem cells[8], lymphocytes[9,10], neutrophils[11,12], neurons[13,14], and cardiomyocytes[15,16]. Here we have explored the role and regulation of Mcl-1 in mammopoiesis.

Results

Mcl-1 expression is dramatically upregulated in luminal cells during lactation

Analysis of Mcl-1 expression revealed that its protein levels varied substantially between the different mammary developmental stages. Profound upregulation of Mcl-1 was evident at the onset of lactation, in contrast to the very low levels of Mcl-1 present at other stages of morphogenesis, based on both immunohistochemical and Western blot analyses (Fig. 1a; Supplementary Fig. 1a). Evaluation of protein expression in freshly sorted cells (Supplementary Fig. 1b,c) from the mammary stem cell (MaSC)-enriched/basal (denoted MaSC/basal; $CD29^{hi}$ $CD24^{+}$) and luminal ($CD29^{lo}CD24^{+}$) cell populations indicated that Mcl-1 upregulation was confined to alveolar luminal cells of the lactating gland and that expression was very low in the MaSC/basal subset across all the development stages (Fig. 1b; Supplementary Fig. 1d,e). Confocal imaging in 3D[17] verified that Mcl-1 protein was induced exclusively in both ductal and alveolar luminal cells at the onset of lactation (Fig. 1c; Supplementary Fig. 2). In contrast to Mcl-1, Bcl-2 was dramatically down-regulated during pregnancy, while Bcl-xL levels remained unchanged through the different developmental stages (Fig. 1b; Supplementary Fig. 1d). Interestingly, *Mcl-1* transcript levels were similar across development by quantitative RT-PCR, with an approximate 2-fold decrease in mRNA levels in luminal cells during lactation (Supplementary Fig. 1f). These data indicate that Mcl-1 expression is subject to post-transcriptional regulation at the onset of lactation. Indeed, there is substantial evidence for post-transcriptional and translational control of Mcl-1 expression in other systems[18-20].

Further fractionation of the luminal population into progenitor and mature subtypes[21] showed that most Bcl-2 pro-survival proteins displayed higher expression in the luminal progenitor

($CD14^+CD61^+$ and $CD14^+CD61^-$) relative to the mature luminal subset ($CD14^-CD61^-$) (Supplementary Fig. 1b,g). Quantitative RT-PCR analysis confirmed *Mcl-1* expression in the different epithelial subpopulations, with lower levels evident in mature luminal cells (Supplementary Fig. 1h).

Loss of Mcl-1 impairs morphogenesis during puberty

To explore the physiological role of Mcl-1 in the mammary gland, we conditionally deleted Mcl-1 at different stages of mammopoiesis (Fig. 2a,b). We first utilized the human *CD4* (hCD4) reporter gene incorporated into the *Mcl-1* allele[22] (Fig. 2a) to monitor *Mcl-1* promoter activity at the single cell level by flow cytometric analysis following *cre*-mediated recombination. CD4 reporter expression could be detected in more than 90% of cells in the MaSC/basal and luminal subsets isolated from K5-cre/*Mcl-1*$^{f/+}$ (Fig. 2c). These results indicate active *Mcl-1* transcription in the vast majority of mammary epithelial cells and efficient recombination at the *Mcl-1* locus by K5-*cre*.

Deletion of *Mcl-1* by either MMTV- or K5-cre was found to profoundly affect ductal morphogenesis during puberty. Only small mammary rudiments were present in 5 week-old MMTV-cre/*Mcl-1*$^{f/f}$ or K5-cre/*Mcl-1*$^{f/f}$ females and by 7 weeks, the ductal trees only half-filled the fat pad, in contrast to littermate control mice (Fig. 2d, e). By 10-12 weeks of age, ductal elongation had largely been rescued, presumably due to continual estrus cycling. The mammary glands of heterozygous (MMTV-cre/*Mcl-1*$^{f/+}$ and K5-cre/*Mcl-1*$^{f/+}$) and *cre*-only mice were indistinguishable from wild-type mice (Fig. 2d,e). Immunostaining for cleaved (activated) caspase 3 revealed a dramatic difference upon *Mcl-1* deletion: there were 0.9% versus 6.5%

cleaved caspase 3-positive cells in the terminal endbuds (TEBs) of control and *Mcl-1*-deficient mammary glands at 6 weeks of age, respectively, with cells in >50 TEBs scored (Fig. 2f; n=4 mice for each genotype; p=0.005, Student's t-test). No difference in the proportion of proliferating, BrdU-positive cells was observed (Fig. 2f), suggesting that Mcl-1 plays a more important role in the regulation of epithelial cell survival as opposed to expansion. In agreement with FACS analysis of hCD4 reporter expression that demonstrated efficient deletion (Fig. 2g), quantitative RT-PCR analysis confirmed a greater than 90% reduction in *Mcl-1* transcript levels (Fig. 2h). The remaining epithelial cells in MMTV-cre/*Mcl-1*$^{f/f}$ glands lacked Mcl-1 expression, indicating that selection against these cells had not occurred.

Loss of Mcl-1 markedly affects stem and progenitor cell activity

Functional analysis of the different mammary epithelial subsets demonstrated that *Mcl-1* deficiency compromised repopulating potential *in vivo* and clonogenic activity *in vitro*. In transplantation assays, the activity of MaSCs (or their direct descendants) from *Mcl-1*-deficient glands was dramatically reduced (Table 1). No outgrowths were generated when cells were transplanted at limiting dilution (100 cells), and only diminutive outgrowths were observed (<10% filling of the fat pad) upon implantation of 400 cells (Fig. 3a). Furthermore, loss of *Mcl-1* severely impaired the clonogenic capacity of both luminal and basal progenitor cells embedded in Matrigel (Fig. 3b). Interestingly, the CD61^{+} luminal progenitor subset was absent from *Mcl-1*-deficient glands while the CD61^{-}CD14^{+} alveolar progenitor subset remained, suggesting differential effects of *Mcl-1* loss on distinct progenitor populations within the mammary gland (Fig. 3c). In order to study the effect of acute deletion of *Mcl-1* on progenitor activity, we isolated epithelial subsets from Rosa26-creER mice for 3D Matrigel cell culture assays. Efficient

Mcl-1 deletion was achieved by treatment with a low concentration of tamoxifen (0.1 μM), and resulted in markedly reduced progenitor activity in both the luminal and MaSC/basal subsets (Fig. 3d,e).

Mcl-1 deficiency affects alveologenesis and impairs lactation

Analysis of mammary glands during pregnancy from either MMTV-cre/*Mcl-1*$^{f/f}$ and K5-cre/*Mcl-1*$^{f/f}$ females indicated an important role in alveolar expansion. The formation of alveolar units was significantly compromised in *Mcl-1*-deficient females at 12.5 and 18.5 days of pregnancy (Fig. 4a-d), as reflected in the presence of small, sparsely distributed alveoli. Apoptosis was augmented following *Mcl-1* deletion, with the appearance of numerous cells positive for cleaved caspase-3 (Fig. 4a-d). The production of milk by the existing alveoli indicated that differentiation was not blocked by *Mcl-1* ablation (Fig. 4d), nor was any change evident in alveolar cell proliferation based on BrdU-immunostaining (Fig. 4c). Nevertheless, neither MMTV-cre/*Mcl-1*$^{f/f}$ nor K5-cre/*Mcl-1*$^{f/f}$ dams were able to nurse their pups, in contrast to heterozygous dams. This resulted in the death of about 70% of pups, lacking milk in their stomachs, within 12 hours after parturition and the remainder within 24 hours.

To specifically address the role of this pro-survival protein during lactation, we used either WAP-icre or an inducible cre to delete *Mcl-1* after formation of the mature alveolar units. The WAP-icre transgene[23] is active in differentiated secretory cells from early lactation. Examination of WAP-icre/*Mcl-1*$^{f/f}$, WAP-icre/*Mcl-1*$^{f/+}$ and Wap-icre dams revealed that pups nursed by WAP-icre/*Mcl-1*$^{f/f}$ dams were significantly stunted, with little milk present in their stomachs (Fig. 5a,b). From 6 days of lactation, the glands showed signs of precocious involution, characterized by the

loss of alveoli, as well as the presence of increased numbers of apoptotic cells positive for activated caspase-3 and for the involution marker pY705 Stat3 (Fig. 5c). No change in proliferating cells was apparent based on Ki67 staining (Fig. 5c), consistent with findings for MMTV-cre and K5-cre-mediated deletion of *Mcl-1* (Fig. 2f). In the second model, Rosa26-creER/ *Mcl-1*$^{f/f}$ dams were treated with tamoxifen immediately after giving birth. By day 5 of lactation, the mammary glands of *Mcl-1*-deficient dams exhibited overt signs of mammary gland involution and no Mcl-1 was detectable in these cells (Fig. 5d). These mice were analyzed prior to them succumbing to other complications such as cardiomyopathy[15,16]. Both of these lactation-specific models underscore the importance of Mcl-1 in maintaining the survival of alveolar luminal cells during lactation.

Identification of EGF as a key growth factor upregulated upon lactation

We next interrogated potential molecular regulators that could mediate the marked induction of Mcl-1 expression that occurs upon lactogenesis. As noted earlier, Mcl-1 expression was induced at the protein but not mRNA level, inferring regulation at the post-transcriptional level. RNA-seq analysis was performed on freshly sorted luminal and basal populations from virgin, 18.5 days pregnant and 2-days lactating mammary glands. Substantial changes in gene expression were observed in the luminal population between late pregnancy and early lactation, whereas expression changes in MaSC/basal cells were smaller and there was little overlap between differentially expressed (DE) genes in the two populations (Fig. 6a). Notably, *Mcl-1* levels were slightly decreased between pregnancy and lactation (Fig. 6b), consistent with qRT-PCR data (Supplementary Fig. 1f). Gene ontology analysis of DE genes showed enrichment for general metabolic processes, lipid biosynthesis and transport proteins in the luminal compartment, and

enrichment for cell contractility genes in the MaSC/basal subset at lactation (Supplementary Table 1), commensurate with the function of the gland at this stage[24]. Gene expression changes in similar functional groups was also observed in microarray studies performed on whole mammary glands[25]. It is noteworthy that there were no significant changes in the transcript levels of E3 ligases and deubiquitinases known to regulate Mcl-1 protein turnover[26,27]. Moreover, no change in the stability of Mcl-1 protein was evident, based on cycloheximide pulse-chase experiments using sorted cell subpopulations (Supplementary Fig. 3a). Thus, the induction of Mcl-1 at lactation appears to be independent of transcriptional or protein stabilization mechanisms.

We hypothesized that the induction of Mcl-1 during lactogenesis could be mediated by a cytokine, growth factor or hormonal cue. The lactogenic hormone prolactin was ruled out since treatment of primary mammary epithelial cell cultures with this hormone led to massive induction of milk synthesis but had no impact on Mcl-1 levels (Supplementary Fig. 3b,c). Notably, *EGF* was the sixth most upregulated gene in luminal cells and the top-ranked of all differentially expressed cytokines and growth factors (Fig. 6b; Supplementary Fig. 4a). Quantitative RT-PCR analysis demonstrated *EGF* mRNA was highly expressed in the luminal cells of lactating glands, with a >100-fold increase between late pregnancy and lactation (Fig. 6c). Further interrogation of the expression of the EGF family of ligands and their receptors revealed that expression of the receptor family was relatively constant while *EGF* was the only ligand induced in luminal cells at lactogenesis (Supplementary Fig. 4b). *Nrg1* and *Nrg2* were equally high in the MaSC/basal population during late pregnancy and lactation, compatible with the basal cell-specific increase in *Nrg1* previously reported[28]. In contrast, betacellulin (*Btc*) and

amphiregulin (*Areg*) were highly expressed in luminal cells at the virgin state but downregulated precipitously during lactation. Thus, *EGF* appears to be exclusively induced at the onset of lactation. It is noteworthy that expression levels of an active form of the EGF receptor (pY1068) were markedly higher upon lactation versus late pregnancy (Fig. 6d). To further explore the effect of EGF on Mcl-1 levels in non-transformed mammary epithelium, a kinetic analysis was performed using HC11 mouse mammary epithelial cells. EGF induced Mcl-1, with protein levels peaking at 2-4 hr post-treatment, before decreasing to lower levels by 16 hr (Fig. 6e). Notably, Mcl-1 was induced in these cells at the protein but not mRNA level (Fig. 6f), and this occurred concomitantly with phosphorylation of EGFR (Fig. 6e).

EGF mediates induction of Mcl-1 translation at the onset of lactation

To formally address whether EGF mediates up-regulation of Mcl-1 during lactation, pregnant dams were treated with lapatinib, a dual inhibitor of EGFR/ErbB1 and ErbB2, or vehicle from 17.5 days of pregnancy. Pups nursed by dams that were administered lapatinib had little milk in their stomachs and were stunted in growth (Fig. 6g), and the mammary glands of pregnant dams exposed to lapatinib underwent precocious involution and had dramatically decreased levels of Mcl-1 (Fig. 6h). Cells positive for cleaved caspase 3 were readily detected within the mammary glands of lapatinib-treated mice mice but were negligible in control glands (Fig. 6h). Given that EGF signalling activates the PI3K/mTOR pathway[29], we investigated whether exposure to EGF results in increased translation of Mcl-1. The mTOR pathway plays a major role in maintaining protein synthesis[30-32] and Mcl-1 has been shown to be translationally regulated by mTOR in certain cancer cells[33,34]. Interestingly, expression of phosphorylated ribosomal protein S6 (pS6)[35], a critical downstream effector of mTOR in the regulation of translation[31], mirrored that of Mcl-1

in mammary epithelial cells during lactation and involution (Supplementary Fig. 5a). Moreover, 3D confocal imaging revealed that high pS6 expression was restricted to alveolar luminal cells of the lactating mammary gland (Supplementary Fig. 5b), and Western blot analysis showed induction of pS6 in EGF-treated HC11 cells (Fig. 6e). In lapatinib-treated mice, expression of pS6 was decreased to virtually undetectable levels (Fig. 6h), suggesting that the EGF pathway modulates mTOR signalling during lactation.

To further explore the involvement of the mTOR pathway in alveolar cell function during lactation, mice were treated with the mTORC1 inhibitor RAD001 (everolimus) from late pregnancy. Blockade of mTOR signalling also resulted in failed lactation and a concomitant decrease in pup weight, accompanied by a dramatic decrease in Mcl-1 and pS6 levels in early lactating glands relative to vehicle-treated mice (Fig. 7a,b). Reminiscent of lapatinib-treated mice, numerous cleaved caspase 3-positive cells were now visible in the mammary glands of RAD001-treated mice (Supplementary Fig. 5c). Compatible with the high levels of pS6, there was a dramatic global increase in protein translation in lactating mammary glands as measured by sucrose density gradient centrifugation (Fig. 7c). Furthermore, analysis of mRNA distribution within these gradients showed that Mcl-1, but not Bcl-X_L, mRNA displayed increased polysome association at both 2 and 4 days of lactation compared to late pregnancy (Fig. 7d; represents averaged data from two biological replicates that are depicted individually in Supplementary Fig. 6). Pertinently, qRT-PCR of *Mcl-1* mRNA extracted from the same samples used for polysome fractionation confirmed that there was no marked increase in *Mcl-1* transcript levels during lactation (Supplementary Fig. 6d,h), consistent with the RNA-seq data. Collectively, these data

suggest that EGF-mediated induction of Mcl-1 at the onset of lactation occurs through mTOR–mediated control of translation.

Discussion

Our data highlight Mcl-1 as a critical regulator of multiple stages of mammary morphogenesis. Mcl-1 regulates the survival of mammary epithelial cells during puberty, pregnancy and lactation. Mcl-1 deficiency at any of these stages resulted in increased numbers of cleaved caspase-3-positive cells, indicative of increased apoptosis. Moreover, Mcl-1 appears to be indispensable for the survival of $CD61^+$ luminal progenitor cells, since this population is absent from *Mcl-1*-deficient mammary glands. Mcl-1 is also likely to have an obligate role in MaSCs since the mammary reconstituting frequency of the MaSC population lacking *Mcl-1* was drastically lower than that of control cells and little fat pad filling was observed even when an outgrowth was generated. However, its precise role in these cells awaits the identification of more refined markers, such as Procr[36], that allow further purification of MaSCs. During lactation, the sole function of alveolar cells is to produce large amounts of milk protein, lipids and other nutrients, a high-energy requirement that places cells under substantial stress. Neither Bcl-w[37] nor Bcl-x[6] play a role in lactation, and Bcl-2 is unlikely to be essential for this process given that its expression decreases markedly upon lactogenesis. Rather, Mcl-1 has emerged as the key pro-survival protein that protects luminal cells from stress-induced cell death during lactation to ensure survival of the offspring.

The profound induction of Mcl-1 at the onset of lactation appears to be largely mediated through *EGF* (Fig. 7e). Even though deletion of *EGF* alone may be dispensable for lactogenesis[38], mice

bearing an EGFR kinase mutation exhibit defective lactation[39], suggesting that compensation by other ligands might occur in the case of germ-line deletion of *EGF*. Other cytokines identified in the gene expression profiling studies, such as IL-15, may also contribute physiologically to the control of Mcl-1 expression. Although our data implicate EGFR/ErbB1, other members of this tyrosine kinase receptor family might be involved in mediating the EGF response through heterodimer formation with ErbB1. For example, ErbB4 deletion in the mammary epithelium has been demonstrated to lead to aberrant differentiation and lactational failure[40,41] and could potentially contribute to EGF-signalling at the onset of lactation.

EGF appears to play a major role in orchestrating the increased translation of Mcl-1 via the mTOR pathway. Inhibition of EGF signalling with lapatinib or the mTOR pathway via RAD001 markedly curtailed lactation. Pertinently, this was accompanied by dramatic decreases in Mcl-1 and phosphorylated ribosomal protein S6, as well as increased numbers of apoptotic cells, further supporting a critical role for EGF-mediated Mcl-1 induction in cell survival. Recently, mTOR inhibitor-mediated suppression of Mcl-1 was implicated in priming rhabdomyosarcoma cells for apoptosis[42]. Notably, polysome fractionation studies on whole mammary glands demonstrated that the translation of Mcl-1 but not Bcl-x was specifically augmented during the transition from late pregnancy to lactation. It is noteworthy that the mechanisms regulating Mcl-1 levels are likely to differ substantively between normal and cancerous cells. EGF was recently shown to transcriptionally regulate *Mcl-1* in certain cancer cell lines via the MAPK pathway[43-45], whereas we have shown here that transcriptional mechanisms do not contribute to the physiological upregulation of Mcl-1 in mammary epithelial cells during lactation.

In contrast to the prominent expression of Mcl-1 in the lactating mammary gland, the level of Mcl-1 protein declines precipitously at the beginning of involution. Presumably down-regulation of this survival factor is required to allow the initiation of apoptosis that has been implicated in the first phase of involution. The exquisite translational regulation of Mcl-1 during mammopoiesis positions it as a crucial regulator of cell survival during lactation and programmed cell death of the alveoli during involution. These findings suggest that Mcl-1 may be the key Bcl-2 family member for the survival of offspring across all mammalian species.

ACKNOWLEDGEMENTS

We are grateful to J. Takeda and M. Takaishi for the kind gift of K5-cre transgenic mice and S. Glaser for provision of mice. We also thank J.L. Clancy, S.K. Archer and G. Duan for assistance with the polysome experiments, B. Helbert for genotyping, and the Animal, FACS, Imaging and Histology facilities at WEHI. This work was supported by the Australian National Health and Medical Research Council (NHMRC) grants #1016701, #1024852, #1086727; NHMRC IRIISS; the Victorian State Government through VCA funding of the Victorian Breast Cancer Research Consortium and Operational Infrastructure Support; and the Australian Cancer Research Foundation. N.Y.F. and A.C.R. and were supported by a National Breast Cancer Foundation (NBCF)/Cure Cancer Australia Fellowship; S.A.B by a NHMRC Postgraduate Scholarship #1017256; P.B., G.K.S., G.J.L. by NHMRC Fellowships #1042629, #490037, #637307; and J.E.V. by an Australia Fellowship.

AUTHOR CONTRIBUTIONS

N.Y.F.: generation and analysis of all mouse models, acquisition and interpretation of major

datasets; N.Y.F., G.J.L. and J.E.V.: experimental design; A.C.R.: confocal imaging; B.P. qPCR analysis; A.L. and G.K.S.: bioinformatic analysis; R.S. and T.P.: polysome fractionation experiments; K.L.: assistance with immunohistochemistry; T.B.: assistance with western blot analysis; S.A.B.: assistance with histological analysis; F.V.: transplantation assays; P.B. and A.S.: provision of Mcl-1 mice and discussions; J.E.V. and N.Y.F. wrote the paper.

COMPETING FINANCIAL INTERESTS

The authors declare no competing financial interests.

1. Hinck, L. & Silberstein, G. B. Key stages in mammary gland development: the mammary end bud as a motile organ. *Breast Cancer Res* **7**, 245-251. (2005).
2. Watson, C. J. Involution: apoptosis and tissue remodelling that convert the mammary gland from milk factory to a quiescent organ. *Breast Cancer Res* **8**, 203 (2006).
3. Kreuzaler, P. A. *et al.* Stat3 controls lysosomal-mediated cell death in vivo. *Nat Cell Biol* **13**, 303-309 (2011).
4. Czabotar, P. E., Lessene, G., Strasser, A. & Adams, J. M. Control of apoptosis by the BCL-2 protein family: implications for physiology and therapy. *Nat Rev Mol Cell Biol* **15**, 49-63 (2014).
5. Moldoveanu, T., Follis, A. V., Kriwacki, R. W. & Green, D. R. Many players in BCL-2 family affairs. *Trends Biochem Sci* **39**, 101-111 (2014).
6. Walton, K. D. *et al.* Conditional deletion of the bcl-x gene from mouse mammary epithelium results in accelerated apoptosis during involution but does not compromise cell function during lactation. *Mechanisms of Development* **109**, 281-293 (2001).

7. Mailleux, A. A. *et al.* BIM regulates apoptosis during mammary ductal morphogenesis, and its absence reveals alternative cell death mechanisms. *Dev Cell* **12**, 221-234 (2007).
8. Opferman, J. T. *et al.* Obligate role of anti-apoptotic MCL-1 in the survival of hematopoietic stem cells. *Science* **307**, 1101-1104 (2005).
9. Opferman, J. T. *et al.* Development and maintenance of B and T lymphocytes requires antiapoptotic MCL-1. *Nature* **426**, 671-676 (2003).
10. Vikstrom, I. *et al.* Mcl-1 is essential for germinal center formation and B cell memory. *Science* **330**, 1095-1099 (2010).
11. Dzhagalov, I., St John, A. & He, Y. W. The antiapoptotic protein Mcl-1 is essential for the survival of neutrophils but not macrophages. *Blood* **109**, 1620-1626 (2007).
12. Steimer, D. A. *et al.* Selective roles for antiapoptotic MCL-1 during granulocyte development and macrophage effector function. *Blood* **113**, 2805-2815 (2009).
13. Arbour, N. *et al.* Mcl-1 is a key regulator of apoptosis during CNS development and after DNA damage. *J Neurosci* **28**, 6068-6078 (2008).
14. Malone, C. D. *et al.* Mcl-1 regulates the survival of adult neural precursor cells. *Mol Cell Neurosci* **49**, 439-447 (2012).
15. Thomas, R. L. *et al.* Loss of MCL-1 leads to impaired autophagy and rapid development of heart failure. *Genes Dev* **27**, 1365-1377 (2013).
16. Wang, X. *et al.* Deletion of MCL-1 causes lethal cardiac failure and mitochondrial dysfunction. *Genes Dev* **27**, 1351-1364 (2013).
17. Rios, A. C., Fu, N. Y., Lindeman, G. J. & Visvader, J. E. In situ identification of bipotent stem cells in the mammary gland. *Nature* **506**, 322-327 (2014).

18. Ertel, F., Nguyen, M., Roulston, A. & Shore, G. C. Programming cancer cells for high expression levels of Mcl1. *EMBO Rep* **14**, 328-336 (2013).
19. Perciavalle, R. M. & Opferman, J. T. Delving deeper: MCL-1's contributions to normal and cancer biology. *Trends Cell Biol* **23**, 22-29 (2013).
20. Thomas, L. W., Lam, C. & Edwards, S. W. Mcl-1; the molecular regulation of protein function. *FEBS Lett* **584**, 2981-2989 (2010).
21. Asselin-Labat, M. L. *et al.* Gata-3 negatively regulates the tumor-initiating capacity of mammary luminal progenitor cells and targets the putative tumor suppressor caspase-14. *Mol Cell Biol* **31**, 4609-4622 (2011).
22. Okamoto, T. *et al.* Enhanced stability of Mcl1, a prosurvival Bcl2 relative, blunts stress-induced apoptosis, causes male sterility, and promotes tumorigenesis. *Proc Natl Acad Sci U S A* **111**, 261-266 (2014).
23. Wintermantel, T. M., Mayer, A. K., Schutz, G. & Greiner, E. F. Targeting mammary epithelial cells using a bacterial artificial chromosome. *Genesis* **33**, 125-130 (2002).
24. Rudolph, M. *et al.* Metabolic regulation in the lactating mammary gland: a lipid synthesising machine. *Physiol Genomics* **28**, 323-336 (2007).
25. Lemay, D. G., Neville, M. C., Rudolph, M. C., Pollard, K. S. & German, J. B. Gene regulatory networks in lactation: identification of global principles using bioinformatics. *BMC Syst Biol* **1**, 56 (2007).
26. Inuzuka, H. *et al.* SCF(FBW7) regulates cellular apoptosis by targeting MCL1 for ubiquitylation and destruction. *Nature* **471**, 104-109 (2011).
27. Schwickart, M. *et al.* Deubiquitinase USP9X stabilizes MCL1 and promotes tumour cell survival. *Nature* **463**, 103-107 (2010).

28. Forster, N. *et al.* Basal cell signaling by p63 controls luminal progenitor function and lactation via NRG1. *Dev Cell* **28**, 147-160 (2014).
29. Hynes, N. E. & Lane, H. A. ERBB receptors and cancer: the complexity of targeted inhibitors. *Nat Rev Cancer* **5**, 341-354 (2005).
30. Ma, X. M. & Blenis, J. Molecular mechanisms of mTOR-mediated translational control. *Nat Rev Mol Cell Biol* **10**, 307-318 (2009).
31. Thoreen, C. C. *et al.* A unifying model for mTORC1-mediated regulation of mRNA translation. *Nature* **485**, 109-113 (2012).
32. Wullschleger, S., Loewith, R. & Hall, M. N. TOR signaling in growth and metabolism. *Cell* **124**, 471-484 (2006).
33. Coloff, J. L. *et al.* Akt-dependent glucose metabolism promotes Mcl-1 synthesis to maintain cell survival and resistance to Bcl-2 inhibition. *Cancer Res* **71**, 5204-5213 (2011).
34. Mills, J. R. *et al.* mTORC1 promotes survival through translational control of Mcl-1. *Proc Natl Acad Sci U S A* **105**, 10853-10858 (2008).
35. Meyuhas, O. Physiological roles of ribosomal protein S6: one of its kind. *Int Rev Cell Mol Biol* **268**, 1-37 (2008).
36. Wang, D. *et al.* Identification of multipotent mammary stem cells by protein C receptor expression. *Nature* **517**, 81-84 (2015).
37. Print, C. G. *et al.* Apoptosis regulator bcl-w is essential for spermatogenesis but appears otherwise redundant. *Proc Natl Acad Sci U S A* **95**, 12424-12431 (1998).
38. Luetteke, N. C. *et al.* Targeted inactivation of the EGF and amphiregulin genes reveals distinct roles for EGF receptor ligands in mouse mammary gland development. *Development* **126**, 2739-2750. (1999).

39. Fowler, K. J. *et al.* A mutation in the epidermal growth factor receptor in waved-2 mice has a profound effect on receptor biochemistry that results in impaired lactation. *Proc Natl Acad Sci U S A* **92**, 1465-1469 (1995).
40. Long, W. *et al.* Impaired differentiation and lactational failure of Erbb4-deficient mammary glands identify ERBB4 as an obligate mediator of STAT5. *Development* **130**, 5257-5268. (2003).
41. Muraoka-Cook, R. S., Feng, S. M., Strunk, K. E. & Earp, H. S., 3rd. ErbB4/HER4: role in mammary gland development, differentiation and growth inhibition. *J Mammary Gland Biol Neoplasia* **13**, 235-246 (2008).
42. Preuss, E., Hugle, M., Reimann, R., Schlecht, M. & Fulda, S. Pan-mammalian target of rapamycin (mTOR) inhibitor AZD8055 primes rhabdomyosarcoma cells for ABT-737-induced apoptosis by down-regulating Mcl-1 protein. *J Biol Chem* **288**, 35287-35296 (2013).
43. Booy, E. P., Henson, E. S. & Gibson, S. B. Epidermal growth factor regulates Mcl-1 expression through the MAPK-Elk-1 signalling pathway contributing to cell survival in breast cancer. *Oncogene* **30**, 2367-2378 (2011).
44. Leu, C. M., Chang, C. & Hu, C. Epidermal growth factor (EGF) suppresses staurosporine-induced apoptosis by inducing mcl-1 via the mitogen-activated protein kinase pathway. *Oncogene* **19**, 1665-1675 (2000).
45. Song, L., Coppola, D., Livingston, S., Cress, D. & Haura, E. B. Mcl-1 regulates survival and sensitivity to diverse apoptotic stimuli in human non-small cell lung cancer cells. *Cancer Biol Ther* **4**, 267-276 (2005).

Figure Legends

Figure 1 Dynamic expression of Mcl-1 protein levels during mammary gland development and involution. (**a**) Immunohistochemical staining for Mcl-1 expression in the mammary glands of FVB/N females at different development stages (n=3 mice per stage). Scale bar: 50 μm. (**b**) Representative Western blot analysis (n=3) of the expression of Bcl-2 family members in sorted luminal ($Lin^-CD29^{lo}CD24^+$) or MaSC/basal ($Lin^-CD29^{hi}CD24^+$) cells isolated from virgin, pregnant (16.5 and 18.5 dP) or lactating (1, 2 and 4 dL) mammary glands of FVB/N mice. SE, short exposure; LE, long exposure. About 50,000 cells were used for each sample. (**c**) 3D whole-mount confocal analysis of Mcl-1 expression in the mammary glands of FVB/N mice at 18.5 days of pregnancy (18.5 dP) or 4 days of lactation (4 dL) (representative of n=3 experiments). Tissues were immunostained for Mcl-1. F-actin was stained by Phalloidin to observe the entire tissue at the cellular level. Scale bars: 30 μm (at 18.5 dP) and 50 μm (at 4 dL).

Figure 2 *Mcl-1* deletion impairs expansion of the mammary epithelium during puberty. (**a**) Schematic diagram of the floxed *Mcl-1* allele. The *Mcl-1* mutant allele contains two loxP sites and the coding sequence for a truncated form of human *CD4* (hCD4). Upon cre-mediated recombination, the hCD4 reporter is expressed on the cell surface. (**b**) The different Cre strains used to delete *Mcl-1* in mammary epithelium. (**c**) Representative FACS plots demonstrating highly efficient recombination at the *Mcl-1* allele (n=4 independent experiments). More than 95% of both luminal and MaSC/basal cells from K5-cre/$Mcl\text{-}1^{f/+}$ females expressed the hCD4 reporter but none could be detected in $Mcl\text{-}1^{f/+}$ mammary epithelial cells. (**d-e**) Whole-mounted mammary glands from 5 or 7 week-old *Mcl-1*-deficient or littermate control mice from the K5-cre (**d**) or MMTV-cre (**e**) model (n=3 mice per genotype). Scale Bars: 2.5 mm. (**f**)

Immunostaining of mammary glands from representative 6 week-old MMTV-cre/*Mcl-1*$^{f/f}$ female and a littermate control for cleaved caspase-3 and BrdU (n=3 independent experiments). Scale bar: 50 μm. **(g)** Representative FACS plots (n=4) demonstrating highly efficient *Mcl-1* deletion from both floxed alleles. Both luminal and MaSC/basal cells from MMTV-cre/*Mcl-1*$^{f/f}$ females display higher hCD4 reporter expression than littermate MMTV-cre/*Mcl-1*$^{f/+}$ females (n=6 mice per genotype). (**h)** Quantitative RT-PCR analysis showing markedly reduced *Mcl-1* transcript levels in the luminal and MaSC/basal populations isolated from individual glands of MMTV-cre/*Mcl-1*$^{f/f}$ mice compared to control mice (mean of 3 technical replicates for each point).

Figure 3 Mcl-l-dependent survival is essential for stem and progenitor cell activity. (**a**) Representative whole-mounts of outgrowths obtained after transplantation of 100 and 400 Lin$^-$ CD29^{hi}CD24$^+$hCD4$^+$ cells isolated from MMTV-cre/*Mcl-1*$^{f/f}$ or control female 10 week-old mice. Less than 5% of the fat pad was filled in the case of MMTV-cre/*Mcl-1*$^{f/f}$ cells (lower right panel). See Table 1. (**b)** Clonogenic activity of the MaSC/basal (Lin$^-$CD29^{hi}CD24$^+$hCD4$^+$) and luminal (Lin$^-$CD29^{lo}CD24$^+$hCD4$^+$) populations (1000 cells) from the mammary glands of 10 week-old MMTV-cre/*Mcl-1*$^{f/f}$ and control mice, grown in Matrigel for 7 days. Scale bars: 0.5 mm. Bar graph showing the % colony forming cells for hCD4$^+$ luminal and basal cells. Data are shown as mean ± SEM for n=3 independent experiments (p=2.54e-11; Student's t-test). (**c)** Deletion of *Mcl-1* results in a diminished CD61$^+$ luminal progenitor subset. Representative FACS plots (n=4) for luminal cells fractionated on the basis of CD61 and CD14 expression. Bar graph (right panel) showing the percentage of each sub-population within the Lin$^-$CD29^{lo}CD24$^+$population isolated from the mammary glands of 10 week-old MMTV-cre/*Mcl-1*$^{f/f}$ or control female mice. Data are shown as mean ± SEM for n=4 mice in each group. p=1.59e-05, Student's t-test for the

change in the $CD61^{+}CD14^{+}$ subpopulation. (**d)** Acute deletion of Mcl-1 *in vitro* using cells from Rosa26-creER mice after treatment of cells with 4-OHT *ex vivo* (n=2 independent experiments). MaSC/basal or luminal populations purified from mice of the indicated genotypes were cultured in Matrigel and analyzed for hCD4 reporter expression at 7 days after induction with 4-OHT for 16 hours. (**e**) Representative images showing the effect of *in vitro* deletion of *Mcl-1* on the activity of 1,500 MaSC/basal or luminal progenitor cells in Matrigel (n=2).

Figure 4 *Mcl-l* deletion impairs alveolar expansion during pregnancy. (**a-d**) Whole-mount analysis and immunostaining for cleaved caspase-3 of mammary glands at 12.5 or 18.5 days of pregnancy from *Mcl-1* deleted or littermate control mice from the K5-cre (**a** and **b**) or MMTV-cre (**c** and **d**) model. For **a-b**, representative images for n=3 mice of each genotype are shown; for **c-d**, the images are representative of n=5 mice. For sections from the MMTV-cre model, immunostaining for BrdU **(c)** and milk **(d)** is also shown (n=3). Scale bars: 1 mm (whole-mount), 50 μm (section).

Figure 5 Ablation of *Mcl-1* in early lactation results in precocious involution. (**a-b**) Reduced growth of pups nursed by lactating WAP-icre/*Mcl-1*$^{f/f}$ dams compared to control littermate females. Pups were weighed every 2 days. Representative photographs of pups are shown in (**a**). (**b**) Body weights of pups were graphed as the mean ± SEM (3 dams per arm with 6 pups each; n=18), yielding a p-value of 1.9e-47, determined using "repeated measures anova." (**c**) H&E sections or immunohistochemical staining of mammary glands from WAP-icre/*Mcl-1*$^{f/f}$ or control dams at 14 days lactation for cleaved caspase-3, Mcl-1, pY705 Stat3 and Ki67 (n=4 mice per genotype). Scale bars: 50 μm. (**d**) H&E sections and immunohistochemical staining for

Mcl-1 in mammary glands from Rosa26-creER/*Mcl-1*$^{f/f}$ or control dams at 5 days of lactation (representative of n=3 mice per genotype). Deletion of the floxed allele was induced with tamoxifen at 0.5 and 2 days post-partum. Scale bars: 50 μm.

Figure 6 EGF mediates up-regulation of Mcl-1 protein at the onset of lactation. (a) Heatmap showing log2-fold changes in MaSC/basal and luminal populations. Populations were sorted from mammary glands at 18.5 days of pregnancy and 2 days of lactation. (**b**) Heatmap of gene expression for *Mcl-1* and cytokines/growth factors that are differentially expressed between late pregnancy and early lactation for the luminal population. Expression values are on a log2 scale and are mean corrected for each gene. Luminal and MaSC/basal cell populations were isolated from virgin, 18.5 days pregnant (18.5 dP) and 2 days lactating (2 dL) mammary glands (FVB/N mice). Two independent sorts from the mammary glands of virgin, pregnant or lactating mice were subjected to RNA-seq analysis. (**c)** Quantitative RT-PCR analysis for *EGF* in the luminal or MaSC/basal population of mammary glands from virgin, 18.5 dP or 2 dL mice. Data are shown as mean ± SEM for n=4 independent mouse samples per genotype. p=8.23e-05 (Student's t-test) for the change between 2 dL vs 18.5 dP luminal cells. **(d)** Immunostaining for pY1068-EGFR in mammary glands at 18.5 dP and 2 dL (n=3 for each). Scale bar: 50 μm. **(e)** Treatment of HC11 mammary epithelial cells with EGF (15 min to 16 h) and Western blot analysis to determine the expression of Mcl-1, pEGFR, pS6 and Actin. Representative blot of three independent experiments. **(f)** Quantification of Mcl-1 protein levels based on western blot analysis and mRNA levels by qRT-PCR for HC11 cells treated with EGF for 2 hrs. Data are shown as mean ± SEM for n=3 experiments. p=0.002; Student's t-test. (**g**) Representative photographs of pups nursed by FVB/N dams administered with lapatinib or vehicle. Arrows

point to milk in the stomachs of pups. Body weights are shown as mean ± SEM (3 dams per arm nursing 6 pups each; n=18). p=9.14e-08 (Student's t-test). **(h)** Immunostaining for Mcl-1, pS6 and cleaved caspase 3 in the mammary glands of mothers administrated lapatinib or vehicle at 2 days of lactation (representative of n=3 independent experiments). Scale bar: 50 μm.

Figure 7 An EGF-mTOR axis mediates up-regulation of Mcl-1 protein via increased translation during lactation. (**a**) Representative photographs of pups nursed by FVB/N dams administered RAD001 (everolimus) or vehicle. Pups were weighed at 5 days of lactation. Body weights were graphed as mean ± SEM (n=3 dams per group). p=7.02e-07. (**b**) Immunostaining for Mcl-1 and pS6 in the glands of mothers administrated RAD001 or vehicle at 5 days of lactation (n=3 dams per arm). Scale bar: 50 μm. (**c)** Extracts from mammary glands from 17 day pregnant (dP), and 2 or 4 day lactating mice (dL) were fractionated by sucrose density gradient centrifugation. Representative polysome profiles (A254: absorbance at 254 nm, dominated by ribosomal RNA) are shown (independent biological repeats shown in Supplementary Fig. 6a,e). An increase of polysomal complexes relative to 80S monoribosomes is indicative of a global increase in protein translation during lactation. (**d)** Distribution profiles of *Mcl-1*, *Bcl-x* and *actin* mRNA in polysome fractions isolated from glands at 17 days of pregnancy (dP), and 2 or 4 days of lactation (dL) were measured by qRT-PCR. Data are presented as averages of two independent biological repeat experiments shown individually in Supplementary Fig. 6c,g. (**e)** Schematic model of EGF/mTOR-mediated up-regulation of Mcl-1 protein in alveolar cells at the onset of lactation.

METHODS

Mice. Mcl-1$^{f/f}$ [22], MMTV–cre (line A)[46] and Rosa26-creER^{T2} (TaconicArtemis) have been previously described and were on mixed FVB/C57Bl/6, FVB/N and C57Bl/6 backgrounds, respectively. Keratin 5 (K5)-cre (C57Bl/6 background)[47] and WAP-icre (FVB/N background)[23] were kind gifts from J. Takeda and G. Schuetz, respectively. For timed pregnancies, adult female mice were mated, scored by the presence of vaginal plugs and confirmed by the examination of embryos at the time of mammary gland collection. For lactation experiments, adult female mice were mated with FVB/N stud males and 6 offspring for each litter were maintained. BrdU (0.5 mg/10 g body weight, Amersham Bioscience) was injected 2 hours prior to mammary gland collection. To inhibit the EGF or mTORC1 pathways, lapatinib (5 mg/mouse, twice per day) or RAD001 (0.5 mg/mouse, daily) were administered respectively by oral gavage, once before birth at 17.5 days of pregnancy and then until collection of glands at 2 days lactation for lapatinib (GlaxoSmithKline) and 5 days lactation for RAD001 (Sigma). Rosa26-creER-mediated deletion of the floxed *Mcl-1* allele was carried out by administering Tamoxifen (3 mg) to lactating mothers at 0.5 and 2 days of lactation by oral gavage. All experiments were conducted with the approval of and according to the guidelines of the Walter and Eliza Hall Institute of Medical Research Animal Ethics Committee.

A minimum of three female mice were analyzed for each genotype and for each developmental time-point. Mice were subjected to the indicated analysis, and the numbers of mice and independent biological experiments are stated in the Figure legends. No statistical method was used to predetermine sample size and the experiments were not randomized. The investigators were not blinded in the analysis of the knockout mice phenotype, as the correct genotype needed

to be studied. In addition, the profound phenotype of knockout animals made blinding impossible. For the drug treatments of mice, all injections were carried out in a blinded fashion by the mouse research technician. The Investigator then removed the mammary glands according to the marking on the boxes that were made by the research technician.

Mammary cell preparation, FACS analysis and cell sorting. Mammary glands were collected from female mice, and single-cell suspensions were prepared as previously described[48]. The following FACS antibodies were used: Biotin-anti-mouse CD14 (rat, clone Sa2-8) from eBioscience; APC/cy7 anti-mouse/rat CD29 (rat, clone HM□1-1), Pacific Blue anti-mouse CD24 (rat, clone M1/69) and PE-anti-mouse/rat CD61 (rat, clone HM63-1) from BioLegend; PE-anti human CD4 (mouse, clone L120) antibodies, APC anti-mouse CD31 (rat, clone MEC13.3), APC anti-mouse CD45 (rat, clone 30-F11), APC anti-mouse Ter119 (rat, clone Ter-119) antibodies from BD PharMingen. To exclude dead cells, cells were re-suspended in approximately 0.2 □g/ml 7-AAD (Sigma) prior to analysis. Cell sorting was performed on the FACS Aria (Becton Dickinson). FACS data were analyzed using FlowJo software (Tree Star, OR, USA). The Lin^- population was defined by $Ter119^-CD31^-CD45^-$.

Histology and whole-mounting of mammary glands. Mammary glands were fixed in 4% paraformaldehyde, embedded in paraffin, sectioned and stained with haematoxylin and eosin (H&E). For whole-mount analysis, mammary glands were fixed in Carnoy's solution containing 60% ethanol, 30% chloroform and 10% glacial acetic acid at room temperature for at least 16 h before staining with carmine alum.

Transplantation and *in vitro* colony forming or differentiation assays. Freshly sorted $CD29^{hi}CD24^{+}hCD4^{+}$ cells from 10-week old mice were implanted into the cleared inguinal glands of 3-week-old syngeneic recipient mice, as described[48]. FACS sorted populations were counted and serially diluted in buffer (40% FCS, 10% Trypan Blue, 25% Growth Factor Reduced Matrigel (BD PharMingen) in PBS) prior to transplantation. Limiting dilution analysis was performed as described[48].

For colony forming assays, sorted mammary luminal or basal cells were embedded in Matrigel (BD PharMingen) as described[48] and cultured for 7–8 days. For deletion of *Mcl-1* in vitro, sorted cells from the mammary glands of Rosa26-creER/*Mcl-1* females were cultured in Matrigel for 24 hours before treatment with 0.1 μM 4-hydroxy-tamoxifen (4-OHT) for 16 hours, followed by culture in normal medium for another 7-8 days. For induction of differentiation and milk production, primary mammary epithelial cells ($Lin^{-}CD24^{+}$) were cultured in Growth Factor Reduced Matrigel for 7 days, starved in serum free medium for 36 hrs before induction with 500 μg/ml hydrocortisone plus 5 μg/ml prolactin in medium containing 2% horse serum for 3 days.

EGF treatment of HC11 cells. HC11 mouse mammary epithelial cells were maintained in RPMI1640 medium containing 2 mM L-glutamine, supplemented with 10% fetal calf serum and 4 μg/ml insulin, 10 ng/ml epidermal growth factor (EGF) and 10 mM HEPES, at 37° C in 5% CO_2. For induction experiments, confluent cells were incubated for 6 hours in RPMI 1640 medium containing 2% horse serum, 4 μg/ml insulin, 500 μg/ml hydrocortisone and 5 μg/ml prolactin, then treated with 100 ng/ml EGF for the indicated time periods.

Cycloheximide pulse-chase experiments. Sorted mammary luminal cells ($Lin^{-}CD29^{lo}CD24^{+}$) from 18.5 day pregnant or 2 day lactating mouse mammary glands were plated in 24-well ultra-low adherence plates (Corning) in mammosphere medium (DMEM/F12 + Glutamax, 1% penicillin/streptomycin, 10 ng/ml bFGF, 5 μg/ml insulin, 500 μg/ml hydrocortisone, B27 supplement) and cultured for 15 min before cells were treatment with 100 μg/ml cycloheximide for different time periods, as described[49]. Cells were collected and analysed by western blotting for Mcl-1 protein levels.

Western blot analysis and immunohistochemistry. FACS-sorted cells were directly lysed in the RIPA buffer containing 1X complete mini protease inhibitor cocktail (Roche) and 1X Roche PhosSTOP phosphatase inhibitor cocktail (Roche). Whole mammary gland lysates were prepared by grinding tissue in liquid nitrogen and solubilizing in RIPA buffer. The following primary antibodies were used for Western blot analysis: anti-Mcl-1 (rabbit, clone D35A5, 1:500 dilution), anti-Bim (rabbit, clone C34C5, 1:500 dilution), anti-Bcl-xL (rabbit, clone 54H6, 1:500 dilution), anti-Stat3 (rabbit, 1:500 dilution), anti-phospho-Stat3 (Tyr705; rabbit, clone D3A7, 1:500 dilution) and anti-phospho-EGFR (Tyr1068, rabbit, clone D7A5, 1:500 dilution) from Cell Signaling; anti-Actin (mouse, clone AC-15, 1:5,000 dilution) and anti-Tubulin (mouse, clone B-5-1-2, 1:5,000 dilution) from Sigma; anti-Bcl-2 (mouse, clone C-2, 1:500 dilution) from Santa Cruz; rat anti-Bcl-w (1:100 dilution) and A1 (1:50 dilution) antibodies were kindly provided by A. Strasser, L. O'Reilly and M. Herold.

Immunohistochemical detection of BrdU-labelled cells was performed as per the manufacturer's protocol using rat anti-BrdU antibody (Accurate Chemical and Scientific and Corporation,

OBT0030G; 1:100 dilution). For other immunohistochemical staining, the following antibodies were used: anti-Mcl-1 (rabbit, clone D35A5, 1:100-400 dilution), anti-pS6 (rabbit, clone D68F8, 1:400 dilution), anti-phospho-Stat3 (Tyr705; rabbit, clone D3A7, 1:100 dilution), and anti-phospho-EGFR (Tyr1068, rabbit, clone D7A5, 1:100 dilution) and anti-cleaved (i.e. activated) caspase-3 (rabbit, clone D3E9, 1:100 dilution) from Cell Signaling. An isotype-matched control IgG was used as the negative control. The streptavidin–biotin peroxidase detection system was used with 3,3'-diaminobenzidine as substrate (DAKO).

For immunohistochemistry and western blot analysis, representative images are shown; the number of independent samples and biological experiments performed is indicated in the Figure legends.

Whole-mount mammary gland preparation for confocal imaging. Tissues were fixed in 4% paraformaldehyde and incubated overnight at 4° C with primary antibody. The following day, tissues were incubated overnight with secondary antibody and phalloidin (1:50; Invitrogen). Tissues were subsequently incubated in 80% glycerol prior to dissection for 3D imaging, as previously described[17]. Primary antibodies: Mcl-1 (rabbit, clone D35A5, Invitrogen; 1:200 dilution), pS6 (rabbit, clone D68F8, Invitrogen; 1:200 dilution) and E-cadherin (rat, clone ECCD-2, Invitrogen; 1:200 dilution). Secondary antibody: anti-rabbit Alexa Fluor 488 (Invitrogen). F-actin was stained with Alexa Fluor 647 Phalloidin (Invitrogen; 1:50 dilution).

Quantitative RT–PCR analysis. Total RNA was prepared from FACS-sorted mammary epithelial subpopulations with the RNeasy Micro kit (Qiagen). Complementary DNA synthesis

and quantitative RT–PCR analysis were performed and normalized against 18S ribosomal RNA, as described previously[50]. See below for qRT-PCR analysis of polysome gradient fractions.

RNA-seq analysis. Total RNA was extracted from sorted luminal or basal populations from the mammary glands of virgin, 18.5 dP and 2 day lactating FVB/N female mice (two independent samples per stage). Total RNA (100 ng) was used to generate libraries for whole transcriptome analysis following the Illumina's TruSeq RNA v2 sample preparation protocol. Libraries were sequenced on an Illumina HiSeq 2000 at the Australian Genome Research Facility (AGRF), Melbourne. At least 20 million 100 bp single-end reads were obtained for each sample. Reads were aligned to the mouse genome mm10 using Rsubread version 13.25[51]. The number of read overlapping each Entrez gene was counted using RefSeq gene annotation and featureCounts[51]. Filtering and normalization used the edgeR package[52]. Genes were filtered as unexpressed if their average count per million (CPM) computed by the aveLogCPM function was less than one. Compositional differences between libraries were normalized using the trimmed mean of M-values (TMM) method (Robinson and Oshlack, Genome Biology 2010). Differential expression analyzed used the Limma package[53]. Counts were transformed to log2-CPM values with associated precision weights using voom[54]. Differential expression was assessed using the TREAT method[55], whereby differential expression is evaluated relative to a biologically meaningful fold-change threshold. Genes were considered to be differentially expressed if they achieved a false discovery rate of 1% in exceeding a fold-change of 1.5. Gene ontology analysis used the goseq package[56], which corrects the analysis for gene length bias. Log-CPM values dispalyed in heatmaps were computed using the edgeR package with a prior.count of 3 to reduce variability at low counts.

Polysome profile analysis. Extracts were prepared from murine mammary glands and polysome fractionation was carried out essentially as described by Stoelzle et al and Clancy et al[57,58] with some modifications. Glands from virgin, late pregnant (d16.5-17.0) or lactating (2 dL and 4 dL) mice (n=2 for each time-point) were flash-frozen in liquid nitrogen and ground to a homogenous powder. Lysis buffer (1 ml of buffer containing 20 mM HEPES (pH 7.6), 125 mM KCl, 5 mM $MgCl_2$, 10 mM DTT, 1% DOC, 1% NP-40, 0.1 mg/mL cycloheximide, 1x cOmplete EDTA-free protease inhibitor cocktail (Roche), 1 mM PMSF, 400 U/mL RNaseOUT™ (Life Technologies) was then added with vortexing. Cell debris was removed from thawed lysates by centrifugation (16,000 g, 10 mins, 4° C). Cleared lysates (approx. 25 A_{260} units) were loaded onto linear sucrose density gradients (17.5-50% (w/v) in lysis buffer w/o detergents, cOmplete inhibitors and RNaseOUT™) and centrifuged for 2h 15min at 35,000g at 4° C in a SW41 Ti rotor (Beckman Coulter). Gradients were displaced from the bottom up by a chase solution (60% sucrose) at a rate of 0.75 mL/min, passed through a UV detector to obtain a continuous A_{254} profile, and collected into 12 fractions using a Brandel BR-188 system at 4° C. Each gradient fraction was spiked with 20 µg of glycogen and 20 pg of an *in vitro* transcribed Renilla Luciferase RNA (3xB RL)[59] and precipitated with 3 volume ethanol overnight at -80° C. After centrifugation RNA was extracted from the pellets with Trizol (Life Technologies) as per the manufacturer's instructions with an additional sodium acetate/ethanol precipitation. The mRNA level of *Mcl-1*, *Bcl-x* and *actin* in each gradient fraction was analysed by quantitative RT-PCR performed on a QuantStudioTM 12K Flex system (Life Technologies) using a Fast SYBR Green Master Mix (Life Technologies). qPCR data from each fraction was first normalized to the 3xB RL spike-in and then expressed as a percentage of total signal across all twelve fractions per gradient. Primer sequences: (5'-3') *Mcl-1 F:* TGTAAGGACGAAACGGGACT, *Mcl-1 R:*

AAAGCCAGCAGCACATTTCT, *BCL-x F:* GACAAGGAGATGCAGGTATTGG, *BCL-x R:* TCCCGTAGAGATCCACAAAAGT, *RL F*: GGCGAGAAAATGGTGCTTGAG, *RL R*: TCCTTGAATGGCTCCAGGTAGG. *Actin* F: CGGTTCCGATGCCCTGAGGCTCTT, *Actin* R: CGTCACACTTCATGATGGAATTGA.

Statistical analysis. Data are shown as Mean ± standard error of the mean (SEM). The Student's t-test was used where applicable, with $p<0.05$ considered significant.

Accession number. RNA-seq data are deposited in Gene Expression Omnibus with accession no. GSE60450.

References

46. Wagner, K. U. *et al.* Cre-mediated gene deletion in the mammary gland. *Nucleic Acids Res* **25**, 4323-4330 (1997).
47. Tarutani, M. *et al.* Tissue-specific knockout of the mouse Pig-a gene reveals important roles for GPI-anchored proteins in skin development. *Proc Natl Acad Sci U S A* **94**, 7400-7405 (1997).
48. Shackleton, M. *et al.* Generation of a functional mammary gland from a single stem cell. *Nature* **439**, 84-88 (2006).
49. Fu, N. Y., Sukumaran, S. K., Kerk, S. Y. & Yu, V. C. Baxbeta: a constitutively active human Bax isoform that is under tight regulatory control by the proteasomal degradation mechanism. *Mol Cell* **33**, 15-29 (2009).

50. Pal, B. *et al.* Global changes in the mammary epigenome are induced by hormonal cues and coordinated by Ezh2. *Cell Rep* **3**, 411-426 (2013).
51. Liao, Y., Smyth, G. K. & Shi, W. featureCounts: an efficient general purpose program for assigning sequence reads to genomic features. *Bioinformatics* **30**, 923-930 (2014).
52. Robinson, M. D., McCarthy, D. J. & Smyth, G. K. edgeR: a Bioconductor package for differential expression analysis of digital gene expression data. *Bioinformatics* **26**, 139-140 (2010).
53. Smyth, G. K. Linear models and empirical bayes methods for assessing differential expression in microarray experiments. *Stat Appl Genet Mol Biol* **3**, Article3. (2004).
54. Law, C. W., Chen, Y., Shi, W. & Smyth, G. K. Voom: precision weights unlock linear model analysis tools for RNA-seq read counts. *Genome Biol* **15**, R29 (2014).
55. McCarthy, D. J. & Smyth, G. K. Testing significance relative to a fold-change threshold is a TREAT. *Bioinformatics* **25**, 765-771 (2009).
56. Young, M. D., Wakefield, M. J., Smyth, G. K. & Oshlack, A. Gene ontology analysis for RNA-seq: accounting for selection bias. *Genome Biol* **11**, R14 (2010).
57. Clancy, J. L. *et al.* Methods to analyze microRNA-mediated control of mRNA translation. *Methods Enzymol* **431**, 83-111 (2007).
58. Stoelzle, T., Schwarb, P., Trumpp, A. & Hynes, N. E. c-Myc affects mRNA translation, cell proliferation and progenitor cell function in the mammary gland. *BMC Biol* **7**, 63 (2009).
59. Pillai, R. S. *et al.* Inhibition of translational initiation by Let-7 MicroRNA in human cells. *Science* **309**, 1573-1576 (2005).

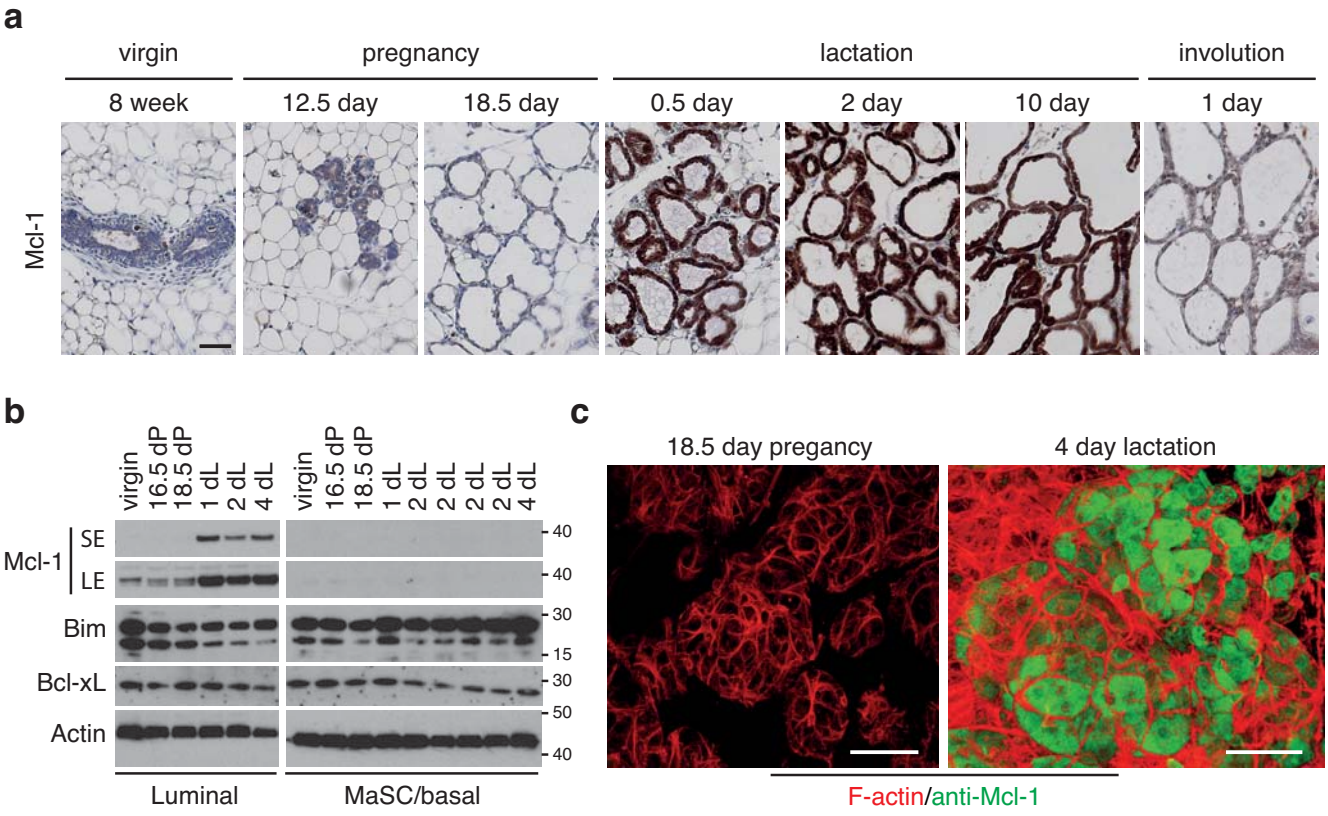
a
virgin
pregnancy
lactation
involution
8 week
12.5 day
18.5 day
0.5 day
2 day
10 day
1 day
Mcl-1
b
virgin
16.5 dP
18.5 dP
1 dL
2 dL
4 dL
Mcl-1
SE
LE
Bim
Bcl-xL
Actin
40
40
30
15
30
50
40
Luminal
MaSC/basal
c
18.5 day pregancy
4 day lactation
F-actin/anti-Mcl-1

Figure 1

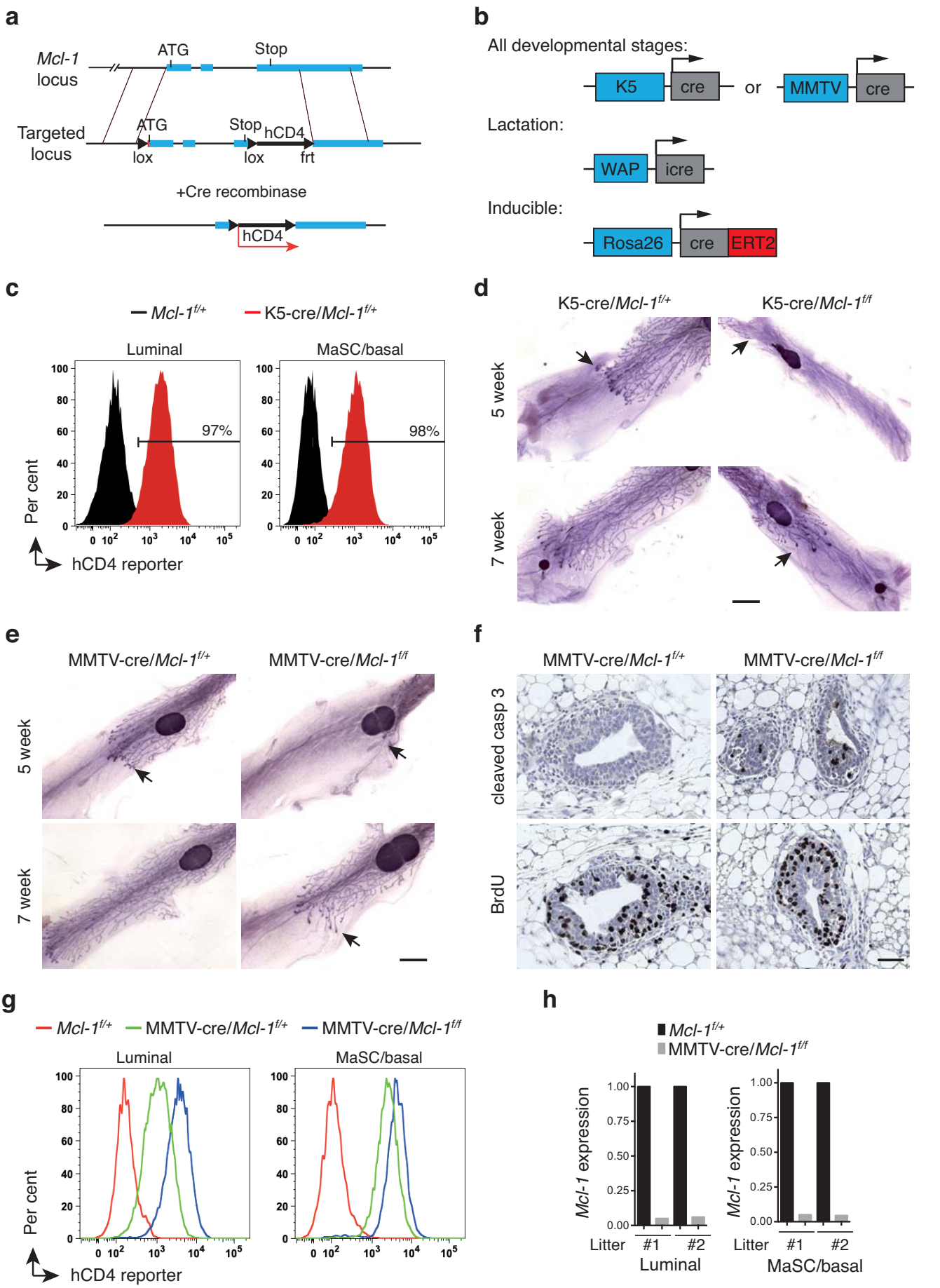
a
Mcl-1 locus
ATG
Stop
Targeted locus
ATG
Stop
hCD4
lox
lox
frt
+Cre recombinase
hCD4
b
All developmental stages:
K5
cre
or
MMTV
cre
Lactation:
WAP
icre
Inducible:
Rosa26
cre
ERT2
c
Mcl-1f/+
K5-cre/Mcl-1f/+
Luminal
MaSC/basal
97%
98%
Per cent
hCD4 reporter
d
K5-cre/Mcl-1f/+
K5-cre/Mcl-1f/f
5 week
7 week
e
MMTV-cre/Mcl-1f/+
MMTV-cre/Mcl-1f/f
5 week
7 week
f
MMTV-cre/Mcl-1f/+
MMTV-cre/Mcl-1f/f
cleaved casp 3
BrdU
g
Mcl-1f/+
MMTV-cre/Mcl-1f/+
MMTV-cre/Mcl-1f/f
Luminal
MaSC/basal
Per cent
hCD4 reporter
h
Mcl-1f/+
MMTV-cre/Mcl-1f/f
Mcl-1 expression
Litter
#1
#2
Luminal
MaSC/basal

Figure 2

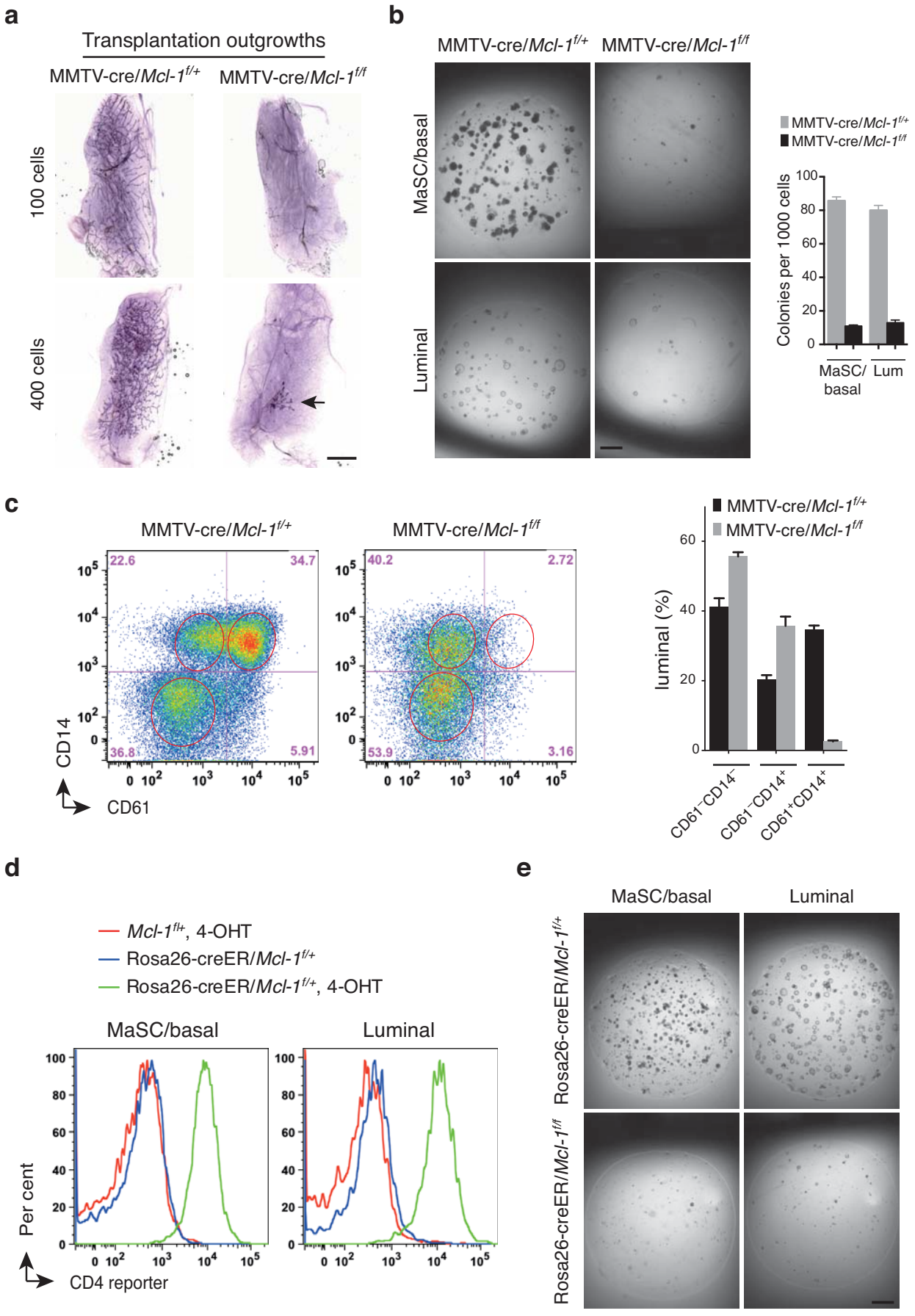
a
Transplantation outgrowths
MMTV-cre/Mcl-1f/+
MMTV-cre/Mcl-1f/f
100 cells
400 cells
b
MMTV-cre/Mcl-1f/+
MMTV-cre/Mcl-1f/f
MaSC/basal
Luminal
MMTV-cre/Mcl-1f/+
MMTV-cre/Mcl-1f/f
Colonies per 1000 cells
100
80
60
40
20
0
MaSC/ basal
Lum
c
MMTV-cre/Mcl-1f/+
MMTV-cre/Mcl-1f/f
22.6
34.7
36.8
5.91
40.2
2.72
53.9
3.16
CD14
CD61
MMTV-cre/Mcl-1f/+
MMTV-cre/Mcl-1f/f
luminal (%)
60
40
20
0
CD61−CD14−
CD61−CD14+
CD61+CD14+
d
Mcl-1fl/+, 4-OHT
Rosa26-creER/Mcl-1f/+
Rosa26-creER/Mcl-1f/+, 4-OHT
MaSC/basal
Luminal
Per cent
100
80
60
40
20
0
CD4 reporter
e
MaSC/basal
Luminal
Rosa26-creER/Mcl-1f/+
Rosa26-creER/Mcl-1f/f

Figure 3

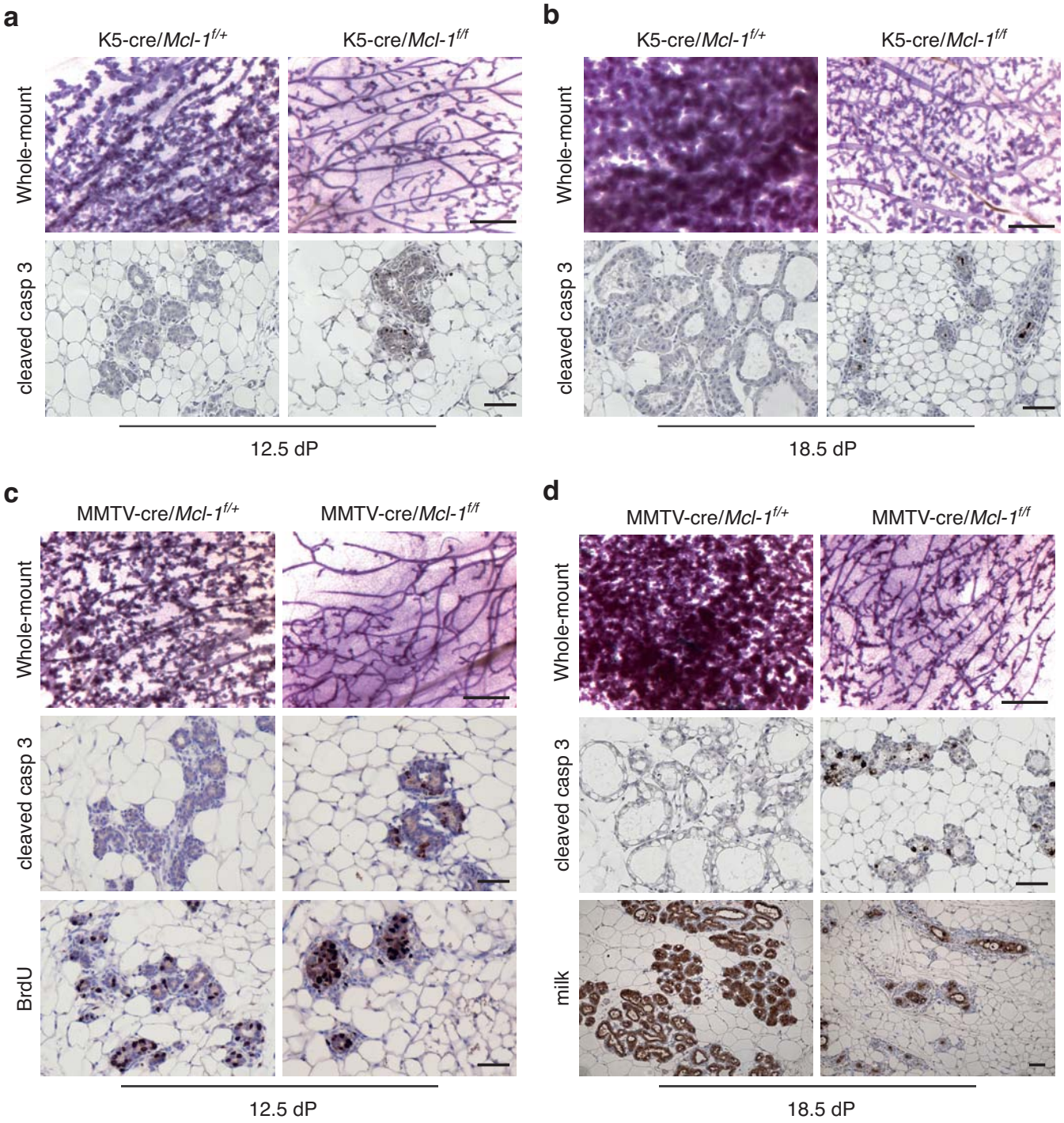
a
K5-cre/Mcl-1f/+
K5-cre/Mcl-1f/f
Whole-mount
cleaved casp 3
12.5 dP
b
K5-cre/Mcl-1f/+
K5-cre/Mcl-1f/f
Whole-mount
cleaved casp 3
18.5 dP
c
MMTV-cre/Mcl-1f/+
MMTV-cre/Mcl-1f/f
Whole-mount
cleaved casp 3
BrdU
12.5 dP
d
MMTV-cre/Mcl-1f/+
MMTV-cre/Mcl-1f/f
Whole-mount
cleaved casp 3
milk
18.5 dP

Figure 4

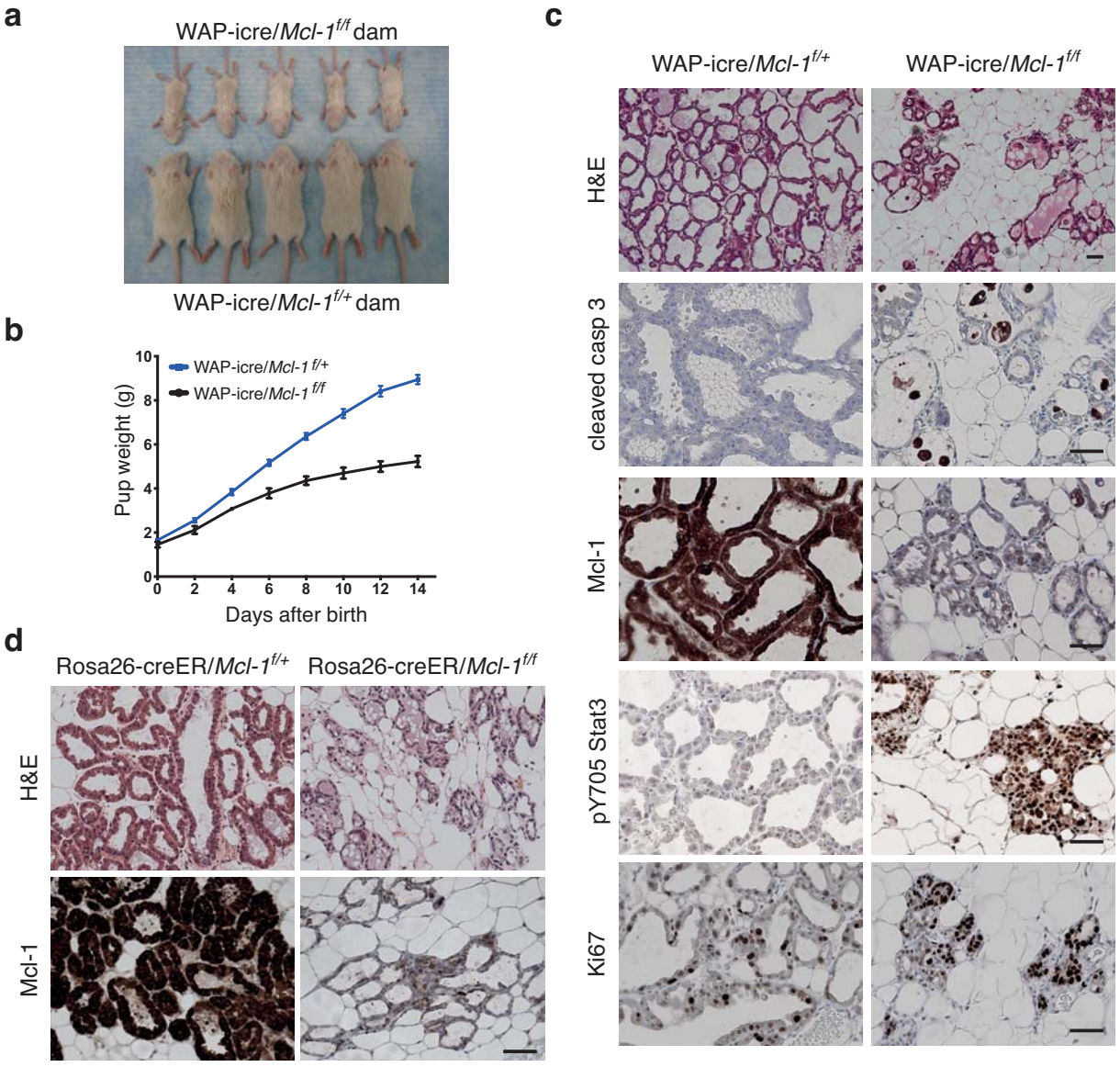
a
WAP-icre/Mcl-1f/f dam
WAP-icre/Mcl-1f/+ dam
b
WAP-icre/Mcl-1 f/+
WAP-icre/Mcl-1 f/f
Pup weight (g)
Days after birth
c
WAP-icre/Mcl-1f/+
WAP-icre/Mcl-1f/f
H&E
cleaved casp 3
Mcl-1
pY705 Stat3
Ki67
d
Rosa26-creER/Mcl-1f/+
Rosa26-creER/Mcl-1f/f
H&E
Mcl-1

Figure 5

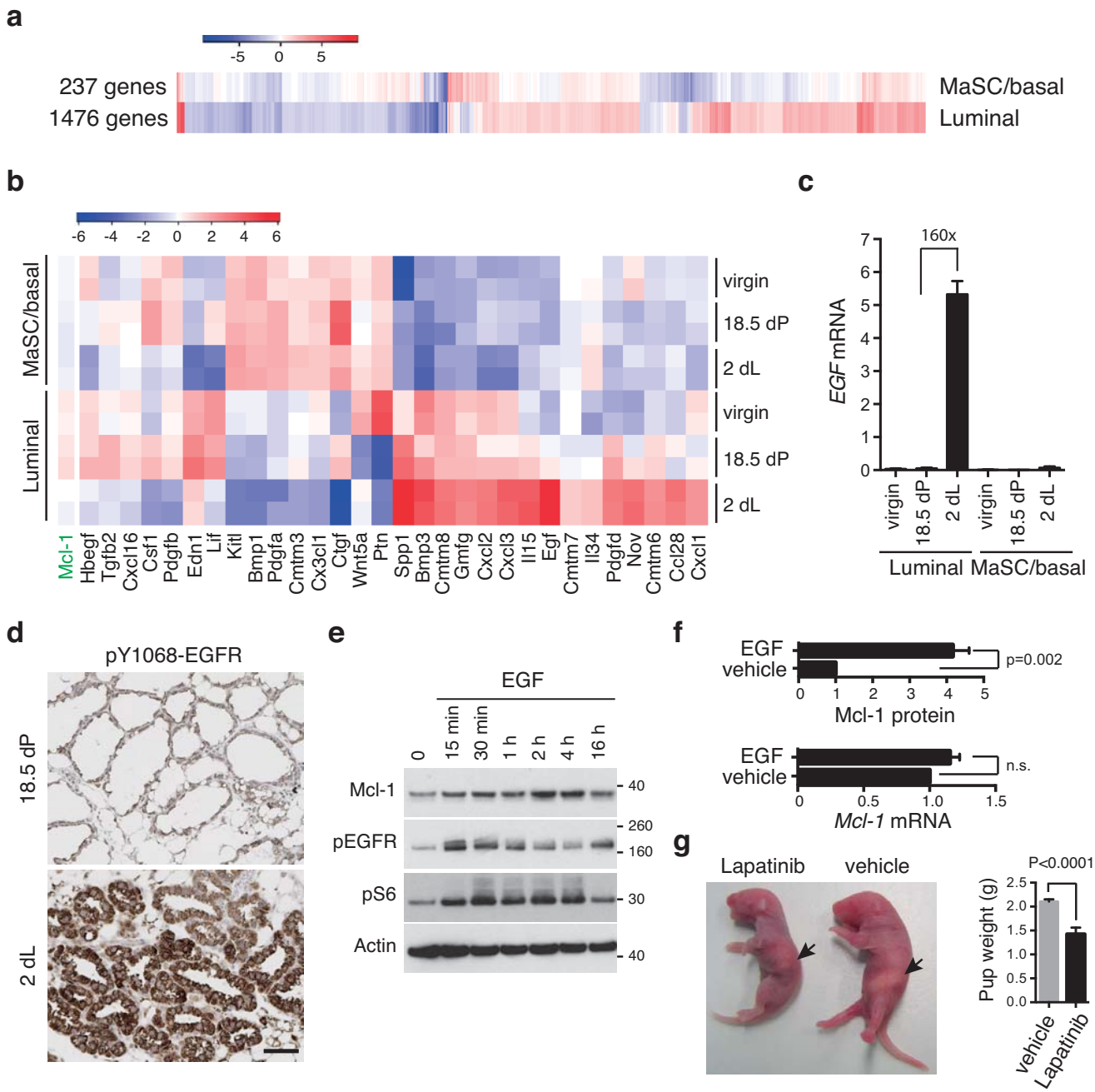
a
-5 0 5
237 genes
1476 genes
MaSC/basal
Luminal
b
-6 -4 -2 0 2 4 6
MaSC/basal
Luminal
virgin
18.5 dP
2 dL
virgin
18.5 dP
2 dL
Mcl-1 Hbegf Tgfb2 Cxcl16 Csf1 Pdgfb Edn1 Lif Kitl Bmp1 Pdgfa Cmtm3 Cx3cl1 Ctgf Wnt5a Ptn Spp1 Bmp3 Cmtm8 Gmfg Cxcl2 Cxcl3 Il15 Egf Cmtm7 Il34 Pdgfd Nov Cmtm6 Ccl28 Cxcl1
c
160x
EGF mRNA
virgin 18.5 dP 2 dL virgin 18.5 dP 2 dL
Luminal MaSC/basal
d
pY1068-EGFR
18.5 dP
2 dL
e
EGF
0 15 min 30 min 1 h 2 h 4 h 16 h
Mcl-1
pEGFR
pS6
Actin
40
260
160
30
40
f
EGF
vehicle
p=0.002
Mcl-1 protein
EGF
vehicle
n.s.
Mcl-1 mRNA
g
Lapatinib
vehicle
P<0.0001
Pup weight (g)
vehicle
Lapatinib
h
Mcl-1
pS6
cleaved casp 3
Lapatinib
vehicle

Figure 6

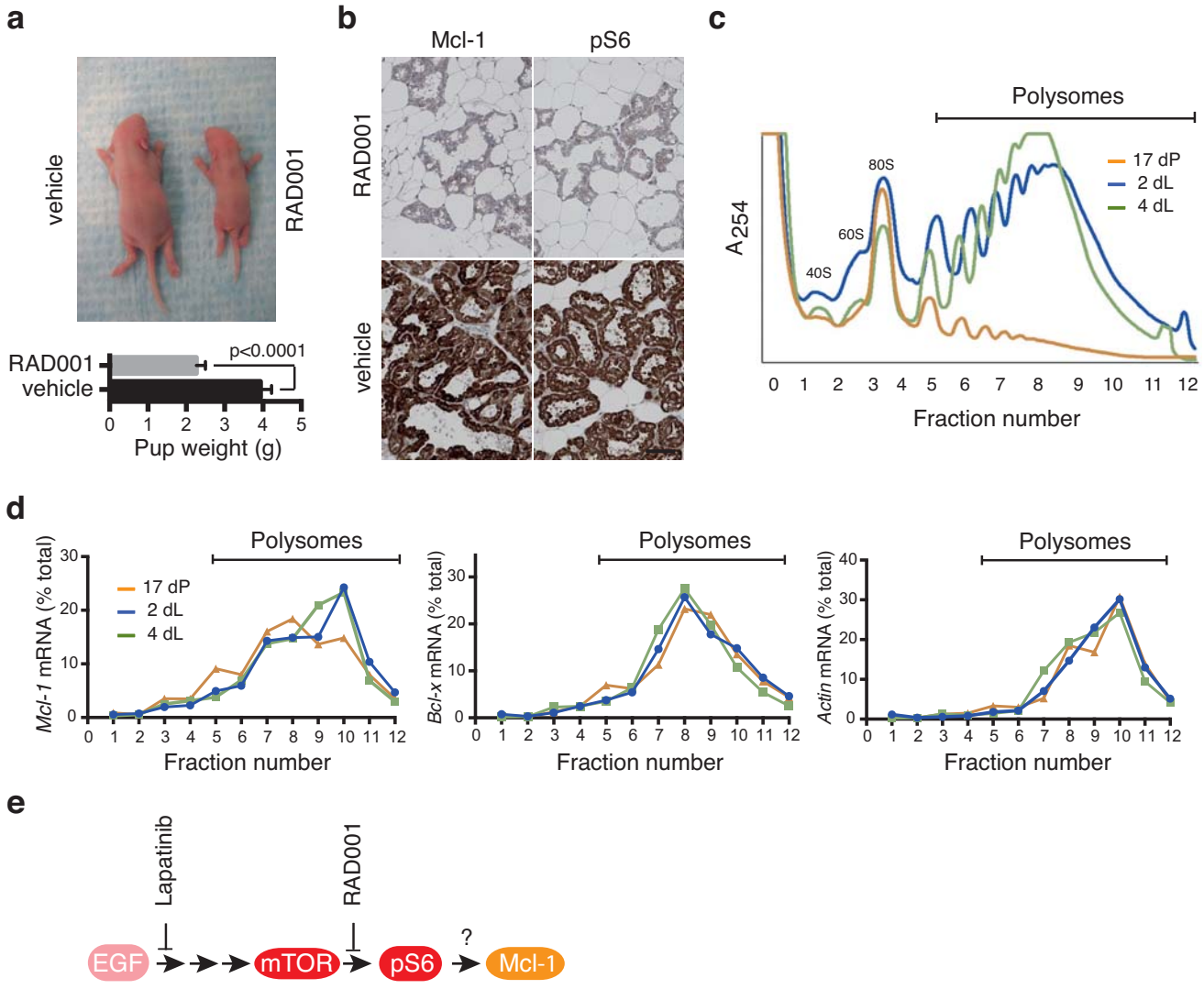
a
vehicle
RAD001
RAD001
vehicle
p<0.0001
0 1 2 3 4 5
Pup weight (g)
b
Mcl-1
pS6
RAD001
vehicle
c
Polysomes
17 dP
2 dL
4 dL
80S
60S
40S
A254
0 1 2 3 4 5 6 7 8 9 10 11 12
Fraction number
d
Polysomes
17 dP
2 dL
4 dL
Mcl-1 mRNA (% total)
0 10 20 30
0 1 2 3 4 5 6 7 8 9 10 11 12
Fraction number
Polysomes
Bcl-x mRNA (% total)
0 10 20 30
0 1 2 3 4 5 6 7 8 9 10 11 12
Fraction number
Polysomes
Actin mRNA (% total)
0 10 20 30 40
0 1 2 3 4 5 6 7 8 9 10 11 12
Fraction number
e
Lapatinib
RAD001
EGF
mTOR
pS6
?
Mcl-1

Figure 7

Table 1: Limiting dilution analysis of the repopulating frequency of MaSC-enriched cells from *Mcl-1*-deficient and control mammary glands.

Genotype	Number of DP cells injected per fat pad	Number of outgrowths*	Repopulating frequency (CI 95%)
MMTV-cre/*Mcl-1*$^{f/f}$	50	0/6	Indeterminant
	100	0/6	
	200	0/6	
	400	0/6	
MMTV-cre/*Mcl-1*$^{f/+}$	50	4/5	1/86 (47-157)
	100	5/6	
	200	6/6	
	400	6/6	

Limiting dilution analysis of the repopulating frequency of MaSC/basal cells from MMTV-cre/*Mcl-1*$^{f/f}$ mice. Freshly sorted Lin^{-}CD29^{hi}CD24^{+}hCD4^{+} (Double Positive, DP) cells from the mammary glands of 10 week-old MMTV-cre/*Mcl-1*$^{f/f}$ or control littermate females were transplanted into the cleared fat pads of 3 week-old recipient mice. *shown as the number of outgrowths per number of injected fat pads. Only outgrowths that filled ≥10% of the fat pad were scored.